



Development of a micro dosing system for fine powder using a vibrating capillary. Part 1: The investigation of factors influencing on the dosing performance

Xiaolong Chen^a, Karlheinz Seyfang^a, Hartwig Steckel^{b,*}

^a Harro Höfliger Verpackungsmaschinen GmbH, Helmholtzstraße 4, 71573 Allmersbach im Tal, Germany

^b Christian Albrecht University Kiel, Department of Pharmaceutics & Biopharmaceutics, Grasweg 9a, 24118 Kiel, Germany

ARTICLE INFO

Article history:

Received 30 January 2012

Received in revised form 24 April 2012

Accepted 25 April 2012

Available online 14 May 2012

Keywords:

Powder
Micro-dosing
Flow rate
Vibration
Frequency
Amplitude
Capillary

ABSTRACT

Precise filling of powder in pharmaceutical development and production is still a challenge, especially when handling small quantities of high potency actives. For this purpose, a micro dosing system for fine powder using a vibrating capillary was developed and investigated. The main objective in this work focused on flow rate and its variability in relation to parameters such as capillary diameter, frequency, and amplitude. The impact of powder properties such as density, particle size, size distribution and shape was also studied with five different kinds of lactose powder. It was found that both the frequency and the amplitude affect the flow rate and variability but with different impact. The range of flow rate can vary from 1 mg to 10 mg per second and a relative standard deviation of better than 3% can be achieved.

© 2012 Elsevier B.V. All rights reserved.

1. Introduction

In the treatment of asthma and COPD, patients are often treated with pre-metered powder doses which might contain one or both of β_2 -agonist and anti-inflammatory glucocorticosteroid. The typical therapeutic dosage of such drugs is in the range of 5–500 μg . For delivery into the deep lung, the drugs are normally micronized or, less frequently, spray dried in order to generate particles with an equivalent aerodynamic diameter smaller than 6 μm . Fine particles tend to agglomerate. Due to this, the operations to fill such small powder quantities into capsules or into blisters are generally very difficult, especially in a commercial scale manufacturing process.

To prevent aggregation and improve their flowability, micronized drug particles are either agglomerated (Hartmann et al., 2009) or blended with larger carrier particles (Frijlink and De Boer, 2004). In latter case, the drug is then de-agglomerated and separated from the carrier by the forces generated during the patient's inhalation. The carrier of choice is α -lactose monohydrate because of its wide availability and in particular its historically good record on safety and tolerability. After the blending the amount to be filled comes up to milligram range and the resulting

powder blends in general have a better flowability compared to the micronized drug. Due to the cohesive nature of bulk material, however, metering the powder in the milligram range is still a challenge.

The main difficulties are caused by the poor flowability of such powders. There are several technical solutions, but to avoid the impact on the powder properties, especially the re-dispersability, vibration was quite often applied to fluidize powder and studied by many research groups in recent decades. Hunt et al. (1999) studied the effects both of horizontal and vertical vibration on powder flow in a hopper. Hickey and Concessio (1994) used a vibrating spatula to characterize the flowability of pharmaceutical powders. However, we focused on the vertical vibration in this study as in common practice the gravitation force is used for the discharge of powder.

The history of using a vibrating capillary to dispense powders began with sand painting. The Navajo Indians drew ceremonial figures with coloured sand. An advanced application in modern industry is in rapid prototyping where fine alloy particles are dosed to generate component parts (Yang and Evans, 2003, 2004). Matsusaka et al. used a vibrating tube to dose powders where the vibration was induced by an ultrasonic transducer (Matsusaka et al., 1995) or a DC motor (Matsusaka et al., 1996). Using the same assembly Ishii et al. (2008, 2009, 2011) characterized different kinds of powder with the focus on their flowabilities. A comparative study of different designs using ultrasonic waves was recently performed by Lu et al. (2009). The authors addressed important process parameters affecting the flow rate and the dosing

* Corresponding author. Tel.: +49 0431 880 13 30; fax: +49 0431 880 13 52.

E-mail addresses: xiaolong.chen@hoefliger.de (X. Chen), karlheinz.seyfang@hoefliger.de (K. Seyfang), h.steckel@pharmazie.uni-kiel.de (H. Steckel).

Table 1
Different setups using a vibrating capillary for powder dosing.

Author/year	Material	Particle size [μm]	$\rho_{\text{particle}}/\rho_{\text{bulk}}$ [kg/m^3]	Actuator	Frequency [Hz]	Amplitude [μm] or [V]
Matsusaka et al. (1995)	Fly-ash	Dp50: 5, 15	2200/-	Ultrasonic transducer	20k (resonance)	N/A
	Alumina	Dp50: 1, 3, 5, 8, 10, 16, 20, 40	4000/-			
	Antimony trioxide	Dp50: 4, 7	5200/-			
	Silicon carbide	Dp50: 0.4	3100/-			
	Clay powder	Dp50: 2	3000/-			
Matsusaka et al. (1996)	Calcium carbonate	Dp50: 2	2800/-	DC-motor	200 (variable)	N/A
	Fly-ash	Dp50: 15	2200/700			
	Alumina (irregular)	Dp50: 6	4000/800			
	Alumina (irregular)	Dp50: 20	4000/1300			
	Alumina (irregular)	Dp50: 10	4000/1600			
Yashchuk et al. (2002)	Silver (spherical)	0–20	10,005/-	Piezoelectric transducer	300–500	450–470 V
Yang and Li (2003)	Copper	3	8900/-	Ultrasonic transducer	49k (resonance)	225 V
Yang and Evans (2003, 2004)	Iron	3	7800/-	Sub-woof loudspeaker	100–300	0–400 μm
	Invar	0–22	8000/-			
	H13 steel	0–212	7800/-			
Jiang et al. (2009)	Fused silica	13.6–30.4	2200/-	Piezoelectric transducer	330 (resonance)	0–130 μm
Lu et al. (2007, 2008, 2009)	Polymethyl-methacrylate (PMMA)	5.2–58.2	1200/-	Ultrasonic transducer	45k (resonance)	30–60 V
	H13 steel	0–22	7800/-			
	Tungsten carbide	12	15,500/-			
Ishii et al. (2008)	Glass beads	42	2300/-	Piezoelectric transducer	330 (resonance)	N/A
	Zirconium oxide	45–850	6000/-			
	Zirconium oxide	0–45, 105–250	7060/-			
Ishii et al. (2009)	Tungsten oxide	0–45, 105–250	7060/-		280 (resonance)	50–160 V

accuracy, such as the frequency and the amplitude. However, the demonstrated correlation between the input parameters and the outcomes were sometimes conflicting (Yang and Evans, 2003; Jiang et al., 2009). This is due to the different experimental setups by the authors and the diverse properties of powder they used (see Table 1). For instance, the material used in these experiments varied from small silver spheres with diameter of 20 μm (Yashchuk et al., 2002) to zirconium oxide with diameters up to 250 μm (Ishii et al., 2008). Most of these applications are in field of rapid prototyping where powders with relative high density are used. However, due to its simple design it is meaningful to consider whether this principle can be applied to dose pharmaceutical powders.

It is well known that pharmaceutical processes seek a more precise dispensing due to the strict regulatory requirements on dose uniformity. With this regard, a micro dosing system for fine powder in the milligram range using a vibrating capillary was developed. According to the literature (Matsusaka et al., 1995; Yang and Evans, 2003, 2004; Lu et al., 2009) and our own assessment, the frequency, the amplitude and the design of the capillary (angle of cone) were taken as input parameters. The flow rate and standard deviation were assessed as output parameters. A factorial experimental design (DoE) was applied to get a better understanding about the correlation between the input parameters and the outcomes. Finally, the dosing system was examined with several commonly used pharmaceutical excipients to verify the influence of particle size and size distribution on the flow rate and the dose variation. The results presented in this publication are limited to different lactose types.

2. Materials and methods

2.1. Machine assembly

A dosing system based on a vibrating capillary was built as shown in Fig. 1.

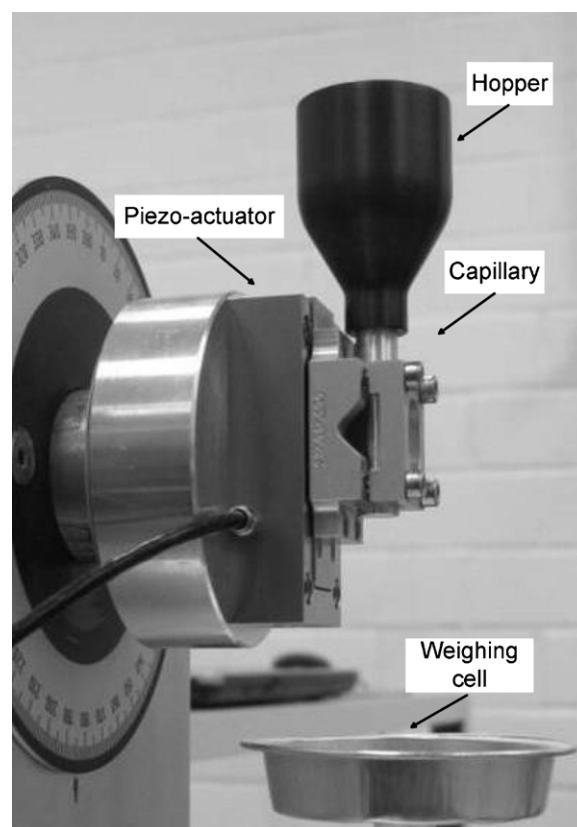


Fig. 1. Close up view of the dosing setup.

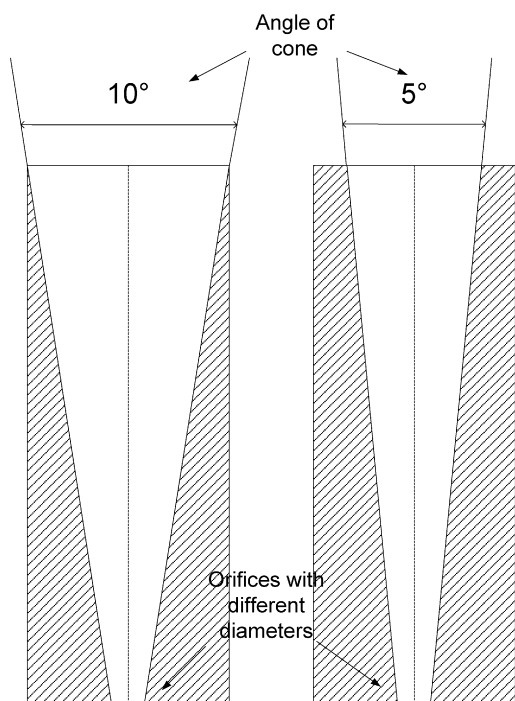


Fig. 2. Designs of the capillaries.

A smaller hopper was connected to the capillary. The capillaries are made of aluminium and their interior wall surfaces are spark-eroded. The designs of capillaries are displayed in Fig. 2. The orifice diameter could vary from 0.5 mm to 2 mm depending on powder properties. However, the capillaries used in this study have an orifice diameter about 0.8 mm and their angles of cone are 10° and 5°, respectively.

The capillary is assembled on a piezo-electric actuator P-753 LISA Linear Actuator (Physik Instrumente, Karlsruhe, Germany). The actuator contains pre-stressed piezo ceramic discs. The working principle is based on the inverse piezo effect, where the application of an electrical field creates mechanical deformation in the crystal. The signal generator 2 MHz Function Generator model 19 (Wavetek, San Diego, USA) and the amplifier LVPZT E501 (Physik Instrumente, Karlsruhe, Germany) are included but not shown in Fig. 1. The signal generator in this study provides three basic wave shapes: the sinusoidal, the rectangular and the triangular wave. An electric signal from 0 V to 12 V is generated by the function generator. Before being applied to the actuator it is boosted 10 times by the amplifier. A weighing cell of type AW-AD (Wipotec, Kaiserslautern, Germany) was connected to the system to assess dose over time and dose accuracy parameters.

2.2. Measurement of the vibration

A laser vibrometer from Polytec (Polytec GmbH, Waldbronn, Germany) was used to characterize the vibration system. As described in Fig. 3, a laser head was pointed to the capillary. The real-time amplitude and the frequency were analysed with Fourier transformation method.

2.3. Powder analysis

The materials used are summarized in Table 2. The Carr's index was taken from the suppliers' specification while the particle size distribution was determined by laser diffraction. The measurement of repose angles (θ°) was conducted with standardized equipment

Table 2

Equivalent spherical volume diameter of powder used and their flow parameters.

Material	X_{10} [μm]	X_{50} [μm]	X_{90} [μm]	Carr's index	θ [°]
Inhalac 70	102.4	205.7	321.9	10.6	35.0
Inhalac 120	88.0	135.2	177.9	11.4	35.4
Inhalac 230	27.7	77.1	123.3	13.4	37.9
Respitose SV 003	34.0	66.2	104.4	19.0	38.7
Flowlac 90	59.2	135.7	222.2	14.9	30.5

according to DIN ISO 4324. The results are taken from the average value of five times repeating.

2.3.1. Laser diffraction scattering method

The volume particle size distribution was measured using a laser diffractometer (Sympatec GmbH, Clausthal Zellerfeld, Germany). Powders were measured in dry form after dispersing in air using compressed air at a pressure of 3 bar (RODOS dispersion module). Particle size distribution was characterized by the X_{10} (the equivalent spherical volume diameter which 10% of the volume in particles is smaller than this), the X_{50} , and the X_{90} value.

2.3.2. Scanning electron microscopy

To get further information about the particle shape and their morphology, SEM pictures were taken using a Philips XL 20 (Philips B.V., Eindhoven, The Netherlands) scanning electron microscope. Samples were fixed on an aluminium stub with conductive double-sided adhesive tape (Leit-Tabs, Plano, Wetzlar, Germany) and coated with gold in an argon atmosphere (50 Pa) at 50 mA for 50 s (Sputter Coater, Bal-Tec, Liechtenstein).

2.4. Experimental procedure

A standardized protocol as described in Fig. 3(a) was applied throughout all experiments: after 500 mg powder was filled into the hopper, the dosing process was initiated by an amplified signal, which started the piezo actuator. The resulting vibration brings the capillary also into oscillation and induces powder flow. A weighing cell records all dosed values and is taken as a feedback unit.

Three dosing regimens described in Fig. 3(b) can be alternately used depending on different requirements. A weighing cell is used in all three regimes but plays different roles. In the method (a) the dose can be simply adjusted by controlling runtime as long as the dose accuracy fulfils the specification. The weighing cell records the powder mass. However, to achieve more precise dose the weighing cell is taken as a feedback unit as in the method (b): the weighing cell delivers the dosed value continuously to a computer. While the actual value is being compared with a given target weight, powders is then dosed until the target weight is obtained. This procedure is very similar to a manual operation. In some case, continuous dosing, as described in method (c) is more appropriate to characterize the flowability of powder where the weighing cell works in a continuous manner. The average difference between every other second approximates the flow rate in milligram per second. The standard deviation of the difference was used to describe the variability of flow rate. The method (c) was applied later in a factorial experimental design. In context of the factorial experiment the dosing procedure with the same parameter setting was repeated twice.

3. Results and discussion

3.1. Mechanical response of dosing system on vibration

As mentioned in Section 1, the vibration applied to the capillary could differ from each other on the vibrating direction, frequency

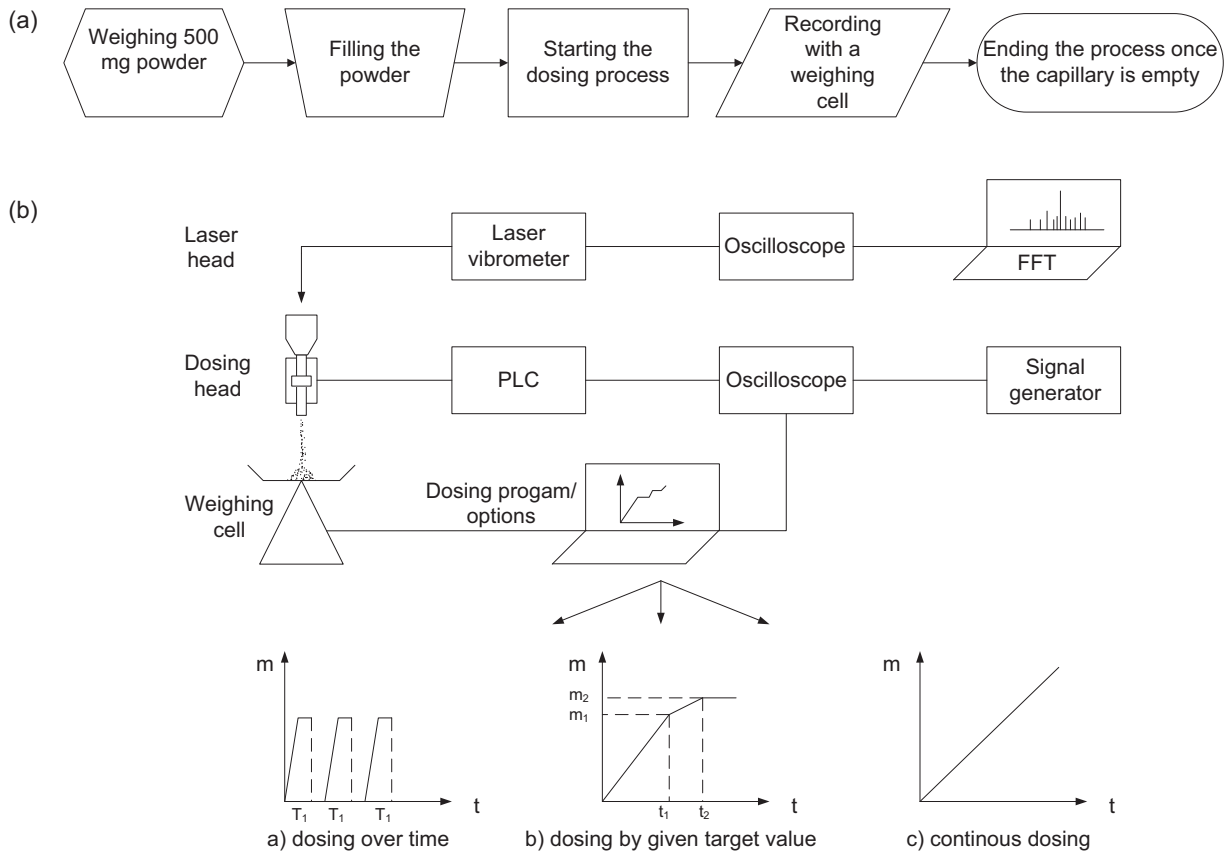


Fig. 3. Experimental procedure and dosing options. (a) Procedure. (b) Dosing options.

and amplitude due to the various types of vibration generators and the mechanical design. Therefore, a precise physical description of the vibration can be helpful in terms of a rational design of experiments. The real-time amplitude and the frequency were recorded in a scanning spectrum as shown in Fig. 4.

Two major conclusions could be drawn by the spectrum analysis. At first, Fig. 4(a) gives evidence of a good linear correlation between the signal by the signal generator and the response of the mechanical body of dosing system: the real amplitude increases directly proportionally with the voltage of the sinus signal. During the amplitude scanning the frequency was held at 1000 Hz. Secondly, while the input voltage was hold at 2 V, the real amplitude changes when the frequency varies as shown in Fig. 4(b). A rapid increase of the amplitude in the spectrum indicates the resonance frequency of the mechanical body. This is different from the application of ultrasonic transducer as the vibration generator where only the single resonance frequency is used. Thus, in order to relieve the dynamical loading on the mechanical structure, the operating window of working frequency was kept lower than the resonance frequency of system. Worth to mention, the actuator (~250 g) applied has a resonance frequency about 5600 Hz ($\pm 20\%$), with a loading about 200 g, the resonance frequency gets lower to 2500 Hz. According to the specification of manufacturer, there is:

$$f'_0 = f_0 \times \sqrt{\frac{M_{eff}}{M_{eff} + M}}$$

where f_0 equals the resonance frequency of actuator, f'_0 equals the resonance frequency of the whole mechanical body, M_{eff} equals one third of the masse of actuator, M equals the loadings on the actuator.

The fill weight of powder material accounts for 5% of the overall loading, therefore, its effect on the resonance frequency is considered as not significant.

On the other side, to initiate the powder flow, the introduced vibration energy must be high enough to overcome the interparticular forces. For a given type of powder, the maximum volume flow rate through an orifice directly proportional correlates to the cross section area. As a summary the following assumptions were made:

- powder does not flow when the frequency or the amplitude or both are below a threshold (critical frequency and critical amplitude),
- the maximum flow rate depends on the capillary orifice, and
- the frequency, the amplitude, and the interaction between them affect the dosing performance.

3.2. Influence of wave shapes on the dosing

As well as the frequency and the amplitude, the wave shape of vibrations could vary. For ease of investigating the influence of wave shapes, the frequency and the amplitude were kept on a constant level. The frequency was set to 900 Hz and the amplitude was hold at 1.5 V. The capillary used has an orifice diameter about 0.8 mm. By switching the function generator, the vibration was changed into a sine wave, a rectangular wave or a triangular wave, respectively. Respirose SV 003 was chosen as an example. The flow rate was estimated by weighing with a weighing cell according to the method (c) described in Section 2.3. The results are displayed in Fig. 5.

This boxplot gives the interquartile range of flow rates. The top line, the middle line and the bottom line indicate the value that 75%,

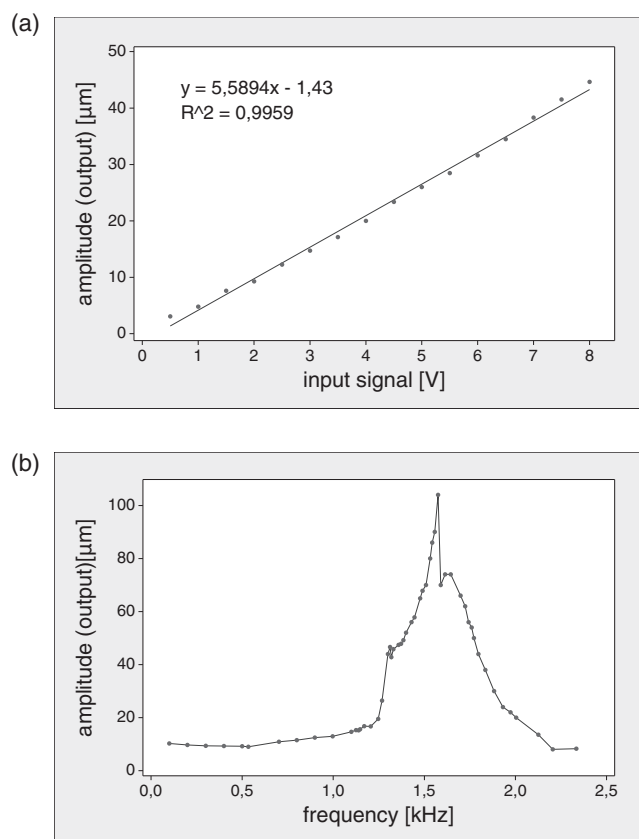


Fig. 4. Mechanical response of the dosing system on vibration. (a) Real amplitude against the input signal. (b) Frequency scanning.

50% or 25% of data are equal or less than this value, respectively. The upper and lower spread bars show the maximum flow rate and the minimum flow rate, respectively.

Compared to the triangular and the rectangular wave the sine wave produced a lower flow rate of about 1.1 mg/s, while the values for the rectangular and the triangular waves were comparable; 5.9 mg/s and 5.8 mg/s, respectively. However, due to the large acceleration and the force loading of non-harmonic waves on the mechanical structure, only the sine wave was applied in the further experiments.

It was found that the flow rate inversely correlated to the increasing amplitude (Staffa et al., 1977; Yang and Evans, 2004). This could be caused by the fact that the vibration they used was

perpendicular to the capillary. According to their simulation, when the horizontal acceleration increased, the collision of particles to the wall increased. This reduced the flow rate while the friction increased. However, the vibration in our experiment was applied at the longitudinal direction of the capillary and produced different results. Thus the orientation of the vibration should be taken in to account.

3.3. Effect of frequency and amplitude on dosing performance

As mentioned above, frequency and amplitude were assumed to be the main influencing factors. In this part, the same capillary with an orifice diameter about 0.8 mm and Respirose SV 003 were used. The results were collected with method (c). The flow rate flow rates and their variability under different parameter settings are displayed in Fig. 6. The flow rate value varied from 0.5 mg/s to 1.5 mg/s. On the left side in Fig. 6, the very low flow rate value shows that the vibration above a certain level (beyond the certain amplitude and frequency) is required to keep powder flowing.

By contrast a high variation of the flow rate on the right side indicates an unstable flow in the state with both high frequency and high amplitude. While the vibration was maintained in vertical direction, it is possible that the vibration propagates differently in some parts of mechanical structure. As a matter of fact, the particles under high input energy can gain velocity not only in the vertical direction. In an observation with a high speed camera, the scattering angle turned broader as the amplitude was raised. It looked like particles “spraying” out of the capillary. The result suggested that a design space should be defined with the vibrating parameters to ensure a stable dosing performance.

3.4. Factorial experimental design: a collective study of the parameters

Design of experiment technique is usually used to minimize the number of experiments required to achieve certain improvement of outputs. In the actual study, the aim was to maximize the flow rate while the accuracy was to be improved. As already discussed, the frequency and the amplitude are the two major factors. In addition, capillaries with two different angles of cone were used in our experiment. Hence, a three-factor, two-level experimental plan was executed according to Table 3.

The flow rate represented the main output parameter. The relative standard deviation was taken as a descriptor of the variability. With regarding to the result in frequency scanning as shown in Fig. 4(b) and to ensure a steady powder flow, the following

Table 3
The factorial experimental design and the results.

Run	Frequency [Hz]	Amplitude [V]	Capillary	Flowrate [mg/s]	RSD [%]
1	1000	10	10°	1.47	17.95
2	1500	10	10°	1.79	4.54
3	1000	4	10°	0.81	7.17
4	1500	4	10°	1.53	4.38
5	1000	4	10°	0.77	7.34
6	1500	4	5°	1.34	33.45
7	1000	10	10°	1.48	4.86
8	1000	4	5°	1.27	12.89
9	1000	10	5°	1.26	25.85
10	1500	10	5°	0.91	29.45
11	1250	7	10°	1.89	5.73
12	1500	4	10°	1.4	17.09
13	1500	10	5°	1.32	29.77
14	1500	4	5°	1.66	4.45
15	1000	4	5°	1.46	8.24
16	1250	7	5°	1.55	23.17
17	1500	10	10°	1.55	2.74
18	1000	10	5°	1.1	16.9

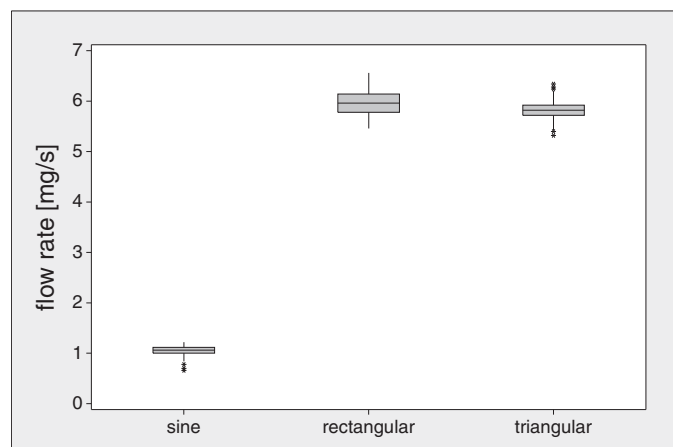


Fig. 5. Comparison of flow rate on vibration with different wave shape.

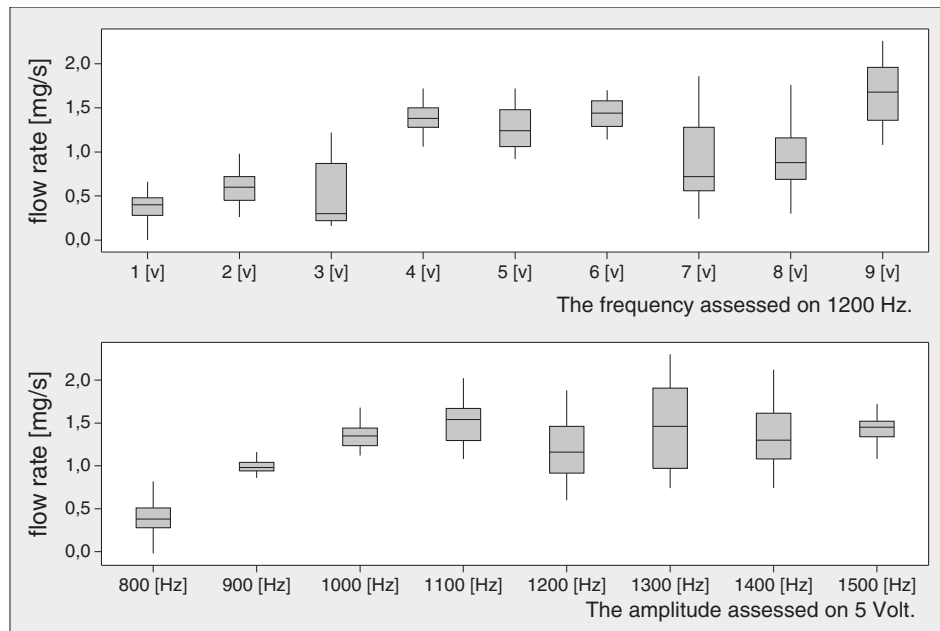


Fig. 6. Influence of frequency and amplitude on the flow rate.

working conditions were taken: amplitude was starting from 4 V up to 10 V; the frequency varied from 1000 Hz to 1500 Hz.

As shown in Fig. 7, the middle points are far from the connecting line between two corners. Hence, the correlation between frequency and amplitude with dose mean and variations cannot be described with a simple linear function. For better understanding, the results are demonstrated in a contour plot as shown in Fig. 8.

The flow rate increases with increasing amplitude, when the frequency is lower than 1200 Hz. Above 1200 Hz the effect of the amplitude is almost negligible. By contrast, the effect of the frequency is even more complicated: at a low level of amplitude: increasing frequency causes an increased flow rate with a high variation. But this trend diminishes when the amplitude was increased to an even higher level.

Taking the results from Section 3.3 into consideration, these results allow for the following conclusions:

- The flow rate can be controlled by changing the input signal,
- compared to the amplitude, the frequency has a predominant effect on the dosing process, and

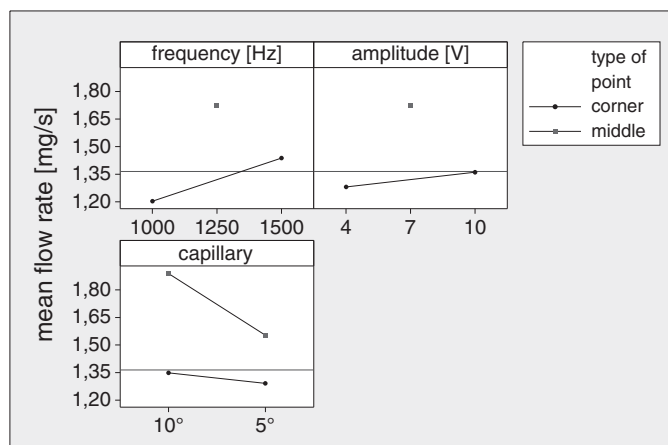


Fig. 7. Major effect of three parameters on the flow rate.

Table 4

Flow rates of different materials in relation to the ratio of the orifice diameter of capillary to the median particle diameter.

Material	Ratio	ρ_{bulk} [g/cm ³]	Flow rate [mg/s]/[mm ² /s]
Inhalac 70	3.4	0.6	5.8/9.7
Inhalac 120	4.2	0.7	9.7/13.9
Inhalac 230	4.9	0.71	3.8/5.4
Respirose SV 003	6.7	0.63	1.8/2.9
Flowlac 90	4.2	0.57	7.4/13.0

- moderate vibration (frequency between 800 Hz and 1200 Hz and amplitude between 2 V and 7 V input voltage) leads to better dosing performance with regarding to the flow rate and its variability.

3.5. Effect of particle size and size distribution on the dosing performance

Not like the frequency and the amplitude, powder properties are a more discrete variation. Particle size and particle size distribution was found to affect the flowability of powder significantly (Ishii et al., 2009). Their influences on the dosing performance were examined with the presented setup. The results were compared with the traditional flowability test methods: the Carr index and the angle of repose tests. The lactose qualities used are listed in Table 2. The capillary used had an orifice with a diameter of about 0.8 mm. The frequency and the amplitude were set on 1200 Hz and 7 V, respectively. The dosing results are shown in Fig. 9.

It is worth mentioning that Inhalac 70 had an irregular flow regime despite its good ranking in Carr's index as well as in the angle of repose tests. The reason is that its coarse particles cannot pass through the capillary orifice uniformly due to the relative small capillary orifice to median particle size ratio, see in Table 4. The ratio is defined as follows: ratio = (diameter of capillary orifice)/(median particle size). For practical purposes the X_{50} value of the samples was taken.

According to the Carr's index values in Table 1, Inhalac 70 should have the highest flow rate among three Inhalac subtypes. However, this is only partly true while comparing the results in Table 4. Indeed, Inhalac 120 produced the maximum flow rate among the three investigated Inhalac subtypes while Inhalac 230 owned the

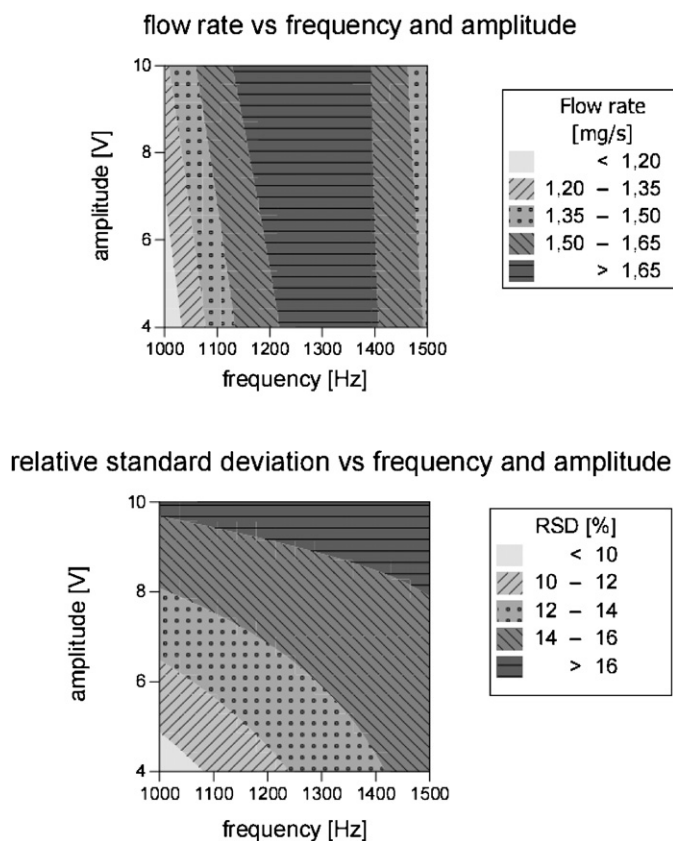


Fig. 8. Diverse trends of flow rates and their variabilities to the frequency and the amplitude.

lowest flow rate. Considering the almost identical bulk density of Inhalac 120 and Inhalac 230, the relative larger surface to particle size of Inhalac 230 should be the substantial cause of its lower flow rate in terms of cohesiveness. Similar results of comparison were confirmed in the measurement of repose angles (see Table 1): Inhalac 230 has the largest angle of repose among three subtypes. Additionally, Flowlac 90 showed better flowability with the smallest angle of repose in Table 2 while its particle size distribution is similar with that of Inhalac 120.

The image analysis also provides the information about the particle size as shown in Fig. 10. Moreover, detailed shape and morphology properties of particles were characterized by the scanning electro-microscopy (SEM). As a good example, the excellent flowability of Flowlac 90 could be explained by the remarkable difference between Flowlac 90 and Inhalac 120 particles. Flowlac 90 has entirely round shape but with shrunken and wrinkled surface while Inhalac 120 owns crystal-like shape and a smooth surface.

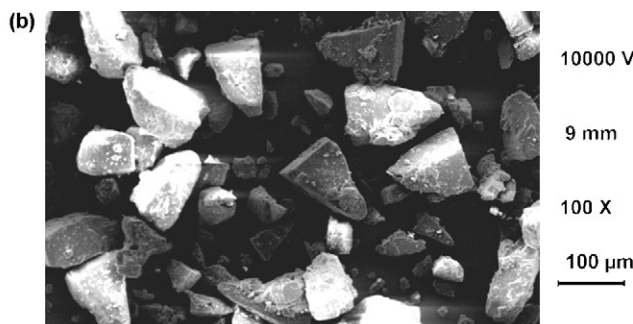
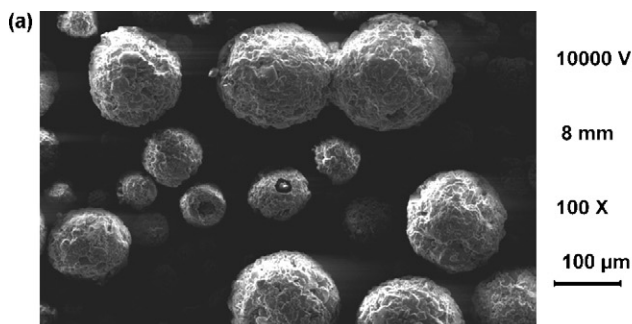


Fig. 10. Morphological difference between (a) Flowlac 90 and (b) Inhalac 120.

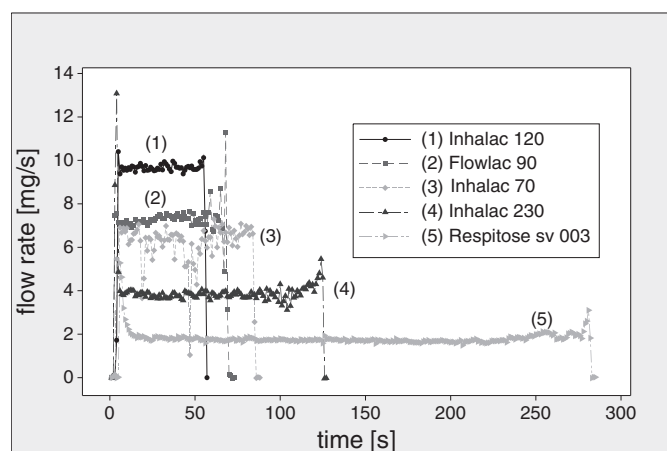


Fig. 9. Comparison of different types of lactose with flow rates as function of time.

Although the flow rates of Flowlac 90 and Inhalac 120 differ significantly from each other, 7.4 mg/s and 9.7 mg/s, respectively, their volumetric flow rates matched each other very well ($13.0 \text{ mm}^3/\text{s}$ and $13.9 \text{ mm}^3/\text{s}$, respectively) due to their similar particle size. Thus, the particle morphology did play a secondary role in this case. However, when the particles size reduces to several micrometres and the cohesive forces like vanderWaals force increases, the separating forces due to the vibration might not be enough to make powder flow.

4. Conclusion

In this study a micro dosing system for fine powder based on a vibrating capillary is discussed. The investigation was focused on the effect of the input parameters on the dosing performance. Frequency and amplitude were found to influence flow rate and its variability while particle size and size distribution of material affect flow rate. With careful adjustment of parameters, the system is able to dose a broad range of pharmaceutical excipients with high precision. The relative compact size could be very helpful in scaling up to multi-unit equipment in terms of minimizing the space requirement. Furthermore, due to the simple design, the developed assembly also make operations easier, for instance, using in aseptic environment (glove box) or dosing of highly potent substances, even using disposable capillaries is also conceivable.

References

- Frijlink, H.W., De Boer, A.H., 2004. Dry powder inhalers for pulmonary drug delivery. *Expert Opin. Drug Deliv.* 1, 67–86.
- Hartmann, T., Mueller, B.W., Steckel, H., 2009. Apparatus and process for continuously producing spherical powder agglomerates. ep2217360 (a1).

- Hickey, A.J., Concessio, N.M., 1994. Flow properties of selected pharmaceutical powders from a vibrating spatula. *Part. Part. Syst. Char.* 11, 457–462.
- Hunt, M.L., Weathers, R.C., Lee, A.T., Brennen, C.E., Wassgren, C.R., 1999. Effects of horizontal vibration on hopper flows of granular materials. *Phys. Fluids* 11, 68–75.
- Ishii, K., Suzuki, M., Segawa, T., Kihara, Y., Yasuda, M., Matsusaka, S., 2011. Flowability measurement of pulverized and granulated materials using vibrating tube method. *Adv. Powder Technol.* 22, 319–323.
- Ishii, K., Suzuki, M., Yamamoto, T., Kihara, Y., Kato, Y., Kurita, T., Yoshimoto, K., Yasuda, M., Matsusaka, S., 2009. Flowability measurement of coarse particles using vibrating tube method. *J. Chem. Eng. Jpn.* 42, 319–324.
- Ishii, K., Suzuki, M., Yamamoto, T., Kihara, Y., Yasuda, M., Matsusaka, S., 2008. Feasibility study on particle flowability evaluation in simplified mox pellet fabrication process using vibrating tube method. *J. Soc. Powder Technol. Jpn.* 45, 290–296.
- Jiang, Y., Matsusaka, S., Masuda, H., Qian, Y., 2009. Development of measurement system for powder flowability based on vibrating capillary method. *Powder Technol.* 188, 242–247.
- Lu, X., Yang, S., Evans, J.R., 2008. Ultrasound-assisted microfeeding of fine powders. *Particuology* 6, 2–8 (Selected Papers from 1st UK–China Particle Technology Forum).
- Lu, X., Yang, S., Evans, J.R., 2009. Microfeeding with different ultrasonic nozzle designs. *Ultrasonics* 49, 514–521.
- Lu, X., Yang, S., Evans, J.R.G., 2007. Dose uniformity of fine powders in ultrasonic microfeeding. *Powder Technol.* 175, 63–72.
- Matsusaka, S., Urakawa, M., Masuda, H., 1995. Micro-feeding of fine powders using a capillary tube with ultrasonic vibration. *Adv. Powder Technol.* 6, 283–293.
- Matsusaka, S., Yamamoto, K., Masuda, H., 1996. Micro-feeding of a fine powder using a vibrating capillary tube. *Adv. Powder Technol.* 7, 141–151.
- Staffa, K.H., Jahn, J., Claussen, N., 1977. Flow ability of powders under influence of vibrations. *Powder Metall. Int.* 9, 20–23.
- Yang, S., Evans, J.R.G., 2003. Computer control of powder flow for solid free forming by acoustic modulation. *Powder Technol.* 133, 251–254.
- Yang, S., Evans, J.R.G., 2004. Acoustic control of powder dispensing in open tubes. *Powder Technol.* 139, 55–60.
- Yang, Y., Li, X., 2003. Experimental and analytical study of ultrasonic micro powder feeding. *J. Phys. D: Appl. Phys.* 36, 1349–1354.
- Yashchuk, V.V., Sushkov, A.O., Budker, D., Lee, E.R., Lee, I.T., Perl, M.L., 2002. Production of dry powder clots using a piezoelectric drop generator. *Rev. Sci. Instrum.* 73, 2331–2335.